Effect of microstructure on spontaneous polarization in amorphous solid water films

Caixia Bu, Jianming Shi, Ujjwal Raut, Emily H. Mitchell, and Raúl A. Baragiola

Citation: The Journal of Chemical Physics **142**, 134702 (2015); doi: 10.1063/1.4916322
View online: http://dx.doi.org/10.1063/1.4916322
View Table of Contents: http://scitation.aip.org/content/aip/journal/jcp/142/13?ver=pdfcov
Published by the AIP Publishing

Effect of microstructure on spontaneous polarization in amorphous solid water films

Caixia Bu,[a] Jianming Shi, Ujjwal Raut, Emily H. Mitchell, and Raúl A. Baragiola
Laboratory for Atomic and Surface Physics, University of Virginia, Thornton Hall, Charlottesville, Virginia 22904, USA

(Received 22 January 2015; accepted 14 March 2015; published online 1 April 2015)

Amorphous solid water (ASW) films grown by vapor deposition below 110 K develop negative surface voltages V_s with respect to the substrate. This polarization is due to a partial alignment of the water molecules during condensation. Kelvin probe measurements show that the magnitude of the surface potential, $|V_s|$, increases linearly with film thickness at a rate that decreases with increasing deposition temperature. $|V_s|$ decreases with increasing deposition temperature and increasing incidence angle of the vapor source. After film growth, $|V_s|$ decreases irreversibly by 80% when the ice film is heated to ~30 K above the deposition temperature. The measurements of $|V_s|$ as a function of film porosity indicate that polarization in ASW is governed by incompletely coordinated water molecules, dangling with unbalanced dipoles at the internal surface of the pores and weakly aligned by the anisotropic film-vacuum interface. This idea is supported by the strikingly similar behavior of $|V_s|$ and the infrared absorption due to the most pliable, two-coordinated surface molecules with annealing temperature. © *2015 AIP Publishing LLC.* [http://dx.doi.org/10.1063/1.4916322]

INTRODUCTION

Water molecules have a balance of "up" and "down" dipoles in regular high-temperature hexagonal ice, providing no net polarization. However, amorphous solid water (ASW), formed by vapor deposition on substrates below ~130 K, becomes spontaneously polarized, showing a negative voltage at the vacuum-ice interface with respect to the substrate. The molecular alignment mechanisms leading to the appearance and growth of polarization have not been explained. Qualitative proposals include resonance energy exchange of the incoming vibrating molecule with the phonons in the condensate[1] and the preferential attraction of protons to the substrate due to an asymmetric distribution of the electric field around the water molecule.[2] The most thorough study of the spontaneous polarization of ASW was done by Iedema *et al.*[3] using a Kelvin probe to measure the surface potentials in the films, referred to as ferroelectricity. We previously confirmed the presence of such intrinsic negative potential on ASW films deposited between 15 and 80 K from the reduced kinetic energies of sputtered secondary ions,[4] using a secondary ion mass spectrometer. While measurements of spontaneous polarization in amorphous ice have been reported for decades,[5,6] a recent study using low-energy electrons incident on ASW remarkably failed to detect polarization in water ice,[7] though it was observed in other condensed polar molecules using the same technique.[8]

Together with small changes in polarization upon crystallization to the cubic phase (>130 K),[2,3,9] the most salient observations pertain to the decrease of the $|V_s|$ with increasing deposition temperature[1,3] and during annealing[3] of ASW films. The thermal relaxation of $|V_s|$, detected previously by Iedema *et al.*,[3] was attributed by them to the "irreversible activation" of the dielectric constant when the film is heated above a temperature higher than previously attained in its thermal history. For instance, they claim that the dielectric constant ε changes from ~2 at 30 K to a large value lying between 37 and 56 at 60 K and that the ε remains large upon subsequent cooling of the ice films.[10] At such large ε, water molecules in the bulk can quickly reorient such that their dipoles shield any preexisting polarization, resulting in a decreased $|V_s|$. However, due to the tetrahedral bonding of water molecules in the bulk, they are unlikely to rotate freely at such low temperatures. Therefore, we propose a more realistic, alternative hypothesis, which is the disappearance of polarization with increasing temperature.

Recent infrared (IR) spectroscopic studies of ASW show absorption features at ~2.7 μm due to O–H stretch vibrations in dangling O–H groups.[11] These weak infrared absorption features, at 3720 cm^{-1} (DB1) and 3696 cm^{-1} (DB2), were assigned to the dangling O–H bonds (DBs) in the two- and three-coordinated water molecules lining the internal surface of the pores, respectively.[12] These two absorption features are insignificant in compact ice but enhanced in ASW films because of the large internal surface area (hundreds of m^2/g)[13] resulting from pores of ~1 nm transverse dimension[14,15] and are used as markers of the ice porosity. In this work, we postulate that the polarization and its thermal behavior are linked to such incompletely coordinated surface molecules. We show the spontaneous polarization of ASW films formed by vapor deposition at 10–110 K and its thermal relaxation, providing evidence for the role of dangling water molecules in the development of film voltage during deposition and its disappearance upon annealing.

[a]Author to whom correspondence should be addressed. Electronic mail: cb8nw@virginia.edu

EXPERIMENTAL DETAILS

Experiments were performed in an ultra-high vacuum (UHV) system with a base pressure of 2×10^{-10} Torr. ASW films were deposited from a collimated vapor beam[16] or from a diffuse background vapor onto a gold-coated quartz crystal microbalance (QCM)[17] cooled with liquid helium. The areal mass of the film was measured by the QCM and converted into column density (in units of monolayers, or ML, defined as 1 ML = 1×10^{15} molecules/cm^2) by dividing by the molecular mass. In some instances, the ice films were also deposited on other substrates such as crystalline ice or transparent CsI. The experimental resolution of the QCM was ~0.08 ML, and the growth rate for all the films was controlled at 0.2 ± 0.1 ML/s. The film thickness d was derived by fitting the Fresnel equations to the interference patterns in the UV-visible optical reflectance.[18] The film density ρ was calculated from the ratio of the column density to the film thickness, and the porosity ($p = 1 - \rho/\rho_c$) was obtained using $\rho_c = 0.94$ g/cm^3 for the density of the intrinsic compact ice.[19]

The system is equipped with a Kelvin probe,[4] which is a non-contact capacitance device with a conductive tip vibrating over the film and measures the contact potential difference (CPD) between the sample and the tip. The surface potential of the film with respect to the substrate was determined from the CPD measurements. The QCM was rotated to face the Kelvin probe to continuously measure the surface potential of the film during deposition of the film from a diffuse background vapor. In the cases when the films were deposited from a collimated vapor beam, the QCM was rotated to face the Kelvin probe for the surface potential measurements immediately after the deposition.

We also collected infrared spectra of ASW films at 2 cm^{-1} resolution in transmission mode with a Nicolet 670 Fourier transform infrared spectrometer installed on a different UHV system. We deposited ice films onto a CsI substrate in the infrared system, different from the gold-coated QCM substrate used for the surface potential measurements. However, as we shall demonstrate below, the substrate does not affect the development of the polarization voltage in ASW films (see Fig. 1 and the related discussion). The infrared spectra were expressed in optical depth, $-\ln(R/R_o)$, where R was the transmission of the film-substrate system and R_o was that of the bare CsI substrate. The integrated absorbance of the two DBs at ~2.7 μm was obtained after subtracting a polynomial baseline fitted to the continuum baseline absorption. We present the dependence of the integrated absorbance of the DBs on annealing temperature and correlate them to the thermal relaxation of surface potential.

RESULTS

Fig. 1 shows that V_s changes abruptly by −0.25 V within the first ~5 ML of deposition from a diffuse background vapor at 30 K and continues to increase linearly in magnitude at a smaller rate with film thickness. The abrupt change in the surface potential observed for thickness <5 ML occurs when ASW is deposited onto a gold (Au) substrate or onto a previously deposited *crystalline* ice film (Fig. 1). The development

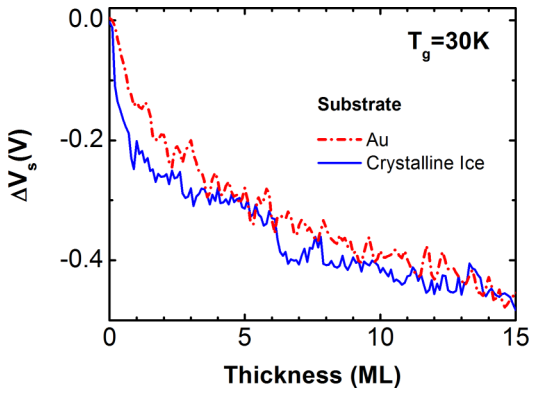

FIG. 1. Evolution of the surface potentials during the first 15 ML of ASW deposition at 30 K and at 0.1 ML/s. The figure shows the change ΔV_s in the substrate potential for different substrates: gold (dashed-dotted line) and gold plus a 538 ML crystalline ice film (solid line).

of the surface potential shows no significant dependence on the substrate material. The abrupt voltage drop in both cases indicates the formation of a dipole layer with the negative charge at the film-vacuum interface.

Fig. 2(a) shows the thickness-dependent evolution of the surface potentials in ASW films. These films were condensed at different deposition temperatures (T_g) from a diffuse vapor source at 0.1 ML/s on the gold substrate. The abrupt development of −0.25 V, similar to the films at 30 K (Fig. 1), was observed in the first ~5 ML in all films for all T_g. Following this initial change, the magnitude of the surface potentials increased linearly with thickness at rates ($\Delta V_s/\Delta L$) that decreased with increasing deposition temperature. Fig. 2(b) shows the rates as a function of growth temperature, in units of

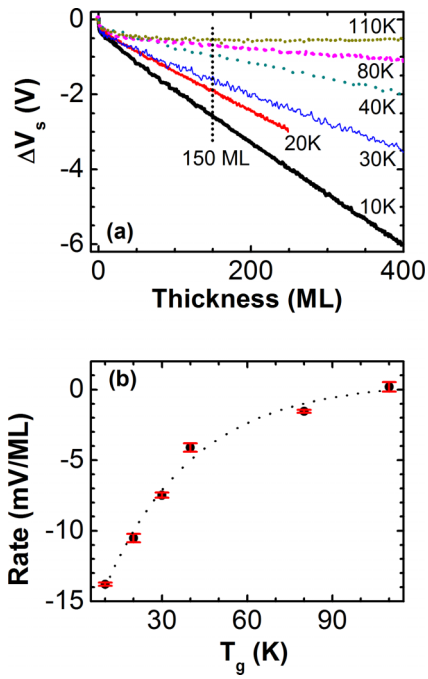

FIG. 2. (a) Variation of the surface potential with ASW film thickness at different deposition temperatures. (b) Rate of change in surface potential ($\Delta V_s/\Delta L$) as a function of deposition temperature (T_g), derived from data in (a) when thicknesses >150 ML.

mV/ML, measured above 150 ML. The absolute value of the rate, $|\Delta V_s/\Delta L|$, decreases with increasing T_g, reaching zero at 110 K. At T_g = 110 K, the film voltage remained approximately constant at the initial value of −0.25 V, not changing with increasing thickness. We observed the same results with an increased growth rate of 0.2 ML/s. This linear behavior also results when the films are deposited from a collimated vapor beam, though the rate depends on the deposition angle, as discussed later.

To ensure that the observed surface potential did not result from co-deposition and/or capture of spurious external charges,[7] we also deposited ASW films onto an electrically biased QCM, floating at positive or negative voltages with respect to the chamber ground to repel stray positive or negative charges, respectively. For 510 ML-thick films grown at 30 K, we obtained the same V_s (within experimental error) when deposited onto the QCM, unbiased or floating at ±10 V, confirming that the observed polarization is intrinsic to the ASW films.

Fig. 3 shows the temperature-dependent evolution of the negative surface potential in ASW films. The ice films, 1100 ML thick, were deposited onto the Au substrate at various temperatures from a collimated vapor beam at normal incidence and then annealed by heating at 4 K/min. We find that $|V_s|$ decreases with increasing T_g and decreases irreversibly by ~80% when the ice film is annealed to a temperature 30 K above T_g. At a particular temperature, we also note that the $|V_s|$ in a film depends on the film's thermal history. For instance, at 60 K, $|V_s|$ in films heated from 10 and 30 K is 1.7 and 4 V, respectively; both are smaller, compared to the 8 V measured in the film following deposition at 60 K. We observe a common feature that if a film is heated from T_g, the surface potential does not decrease immediately but lags for ~4 K above the T_g. A likely explanation is the transient increase in the local temperature at the sticking point due to the formation of new hydrogen bonds.

The thermal depolarization shown in Fig. 3 was also observed by Iedema *et al.*[3] for films grown at $T_g \geq 40$ K and was explained by dipole shielding (discussed in the Introduction), which required a drastically increased dielectric constant ε, even at temperatures below 100 K. To test this hypothesis, we performed charging/discharging experiments on the ice films using 500 eV He^+ ions. The films (1100 ML) were deposited at 30 K, annealed to different temperatures (T_a = 60, 80, 120, and 140 K) and cooled back to 30 K prior to ion exposure. The significant increase in ε, as proposed by Iedema *et al.*,[3] would have occurred in the first annealing cycle. The films would also have retained a high ε upon subsequent cooling to 30 K, as changes in ε are irreversible.

Irradiation at 500 eV He^+ leads to an accumulation of positive charge at the top few MLs of the film surface and minimal sputtering (less than 0.01% of the total mass of the film). The charge per unit area deposited by the He^+ ions is equal to F, the irradiation fluence measured with a Faraday cup. When all ions are on top of a dielectric film on a grounded substrate, the resulting surface potential V_s, measured using the Kelvin probe, is $V_s/F = d/(\varepsilon\varepsilon_o)$, where ε_o is the vacuum permittivity and ε is the dielectric constant of the film. If the hypothesis proposed by Iedema *et al.* was correct, ASW films annealed to higher T_a in the first annealing cycle would have larger values of ε and consequently smaller values of V_s/F. However, Fig. 4 shows that $V_s/F = d/(\varepsilon\varepsilon_o)$ is roughly constant (within 15% of the average value) following charge deposition at 30 K. This observation disproves the claim of high ε at low temperatures; instead, it establishes that ε remains approximately constant at ~3 (±0.6) over 30–140 K,[20] since changes in d with temperature in the first annealing cycle are nominal, <12%.[21] We notice that the V_s sharply decreases during the second annealing cycle when the temperature exceeds the T_a reached in the first annealing cycle (Fig. 4). We attribute this to charge leakage to the substrate; it will be discussed in more detail in a future publication.[20]

We now introduce into the discussion with porosity ($p = 1 - \rho/\rho_c$) a salient feature in ASW films, in efforts to find an alternative hypothesis to explain the observed thermal depolarization that does not require a temperature-dependent ε. That the porosity of ASW decreases with increasing deposition and annealing temperature[13,22] shows trends similar to the thermal

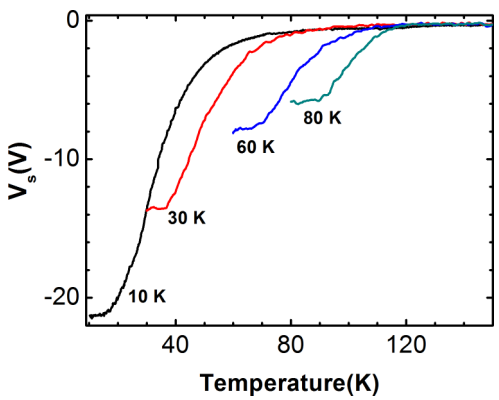

FIG. 3. The decay of polarization with annealing temperature for 1100 ML ASW films grown at temperatures between 10 and 80 K.

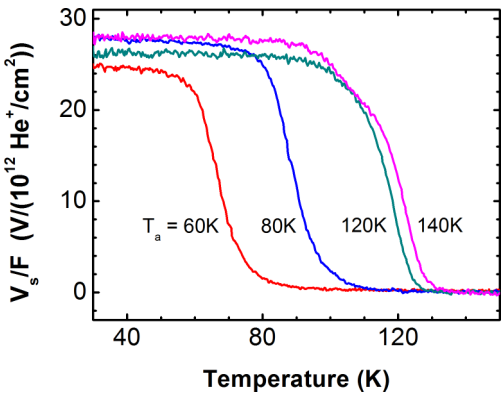

FIG. 4. Surface voltages for ASW films charged by 500 eV He^+. The graph shows the temperature dependence of the ratio of surface potential to surface charge density (ion fluence), $V_s/F = d/\varepsilon\varepsilon_o$, for films pre-annealed at T_a = 60 K, 80 K, 120 K, and 140 K. The ASW films were deposited at 30 K, pre-annealed at T_a = 60 K, 80 K, 120 K, and 140 K and then cooled to 30 K before depositing charge. The films were charged to ~17 V with a fluence $(0.62 \pm 0.09) \times 10^{12}$ He^+/cm^2. The ratio $V_s/F = d/\varepsilon\varepsilon_o$ is seen to be relatively independent of temperature before dropping sharply at temperatures greater than the pre-annealing temperatures. This drop is attributed to the leakage of charge to the substrate.

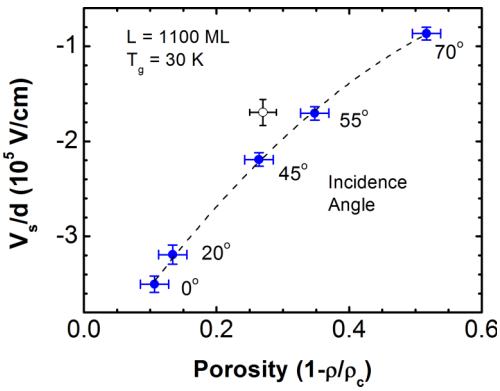

FIG. 5. Dependence of internal polarization field on porosity. Labels are the incidence angle of the vapor flow. The black-circle data point is for the deposition from a diffuse background source at 30 K. The dashed line is to guide the eye.

evolution of the polarization voltage $|V_s|$, leads us to explore the link between polarization and porous microstructure in ASW films. We would expect that $|V_s|$ increases with porosity, based on the decreasing effects of temperature (growth and annealing) on both porosity[13,22] and $|V_s|$ (Figs. 2 and 3). Besides temperature, another method to modify ASW porosity is by varying the deposition angle θ when films are condensed from a collimated vapor source,[14,15] and the porosity increases at higher incidence due to shadowing effects.[23] Thus, to further evaluate the correlation between porosity and polarization, we deposited ASW films with a collimated vapor beam at various incidence angles θ at 30 K and expected $|V_s|$ to increase with θ. However, experimental results show that the magnitude of the internal polarization field (IPF) decreases with increasing θ and therefore porosity (Fig. 5). The IPF is obtained by dividing the film voltage by its thickness (V_s/d), a useful normalization since films with the same areal mass but different porosities have different thicknesses. The contrast between the expected and measured polarization as a function of deposition angle points to additional effects at non-normal incidences, which we address later.

Fig. 6 shows the decay of the IPF with annealing temperature for ASW films (1100 ML) deposited at 0°, 45°, and 70°

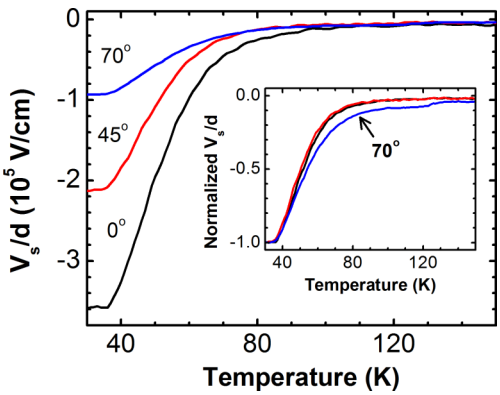

FIG. 6. The decay of the internal polarization fields with annealing temperature for 1100 ML ASW films deposited at different incidences at 30 K. Inset: the normalized curves show the distinct behavior of films grown at 70°, which have mesopores in addition to nanopores.

at 30 K. We normalize the IPF to its initial value at 30 K in the inset of Fig. 6. Upon annealing to 80 K, the IPF decreases to ~5% of the initial value for the films deposited at 0° and 45°. The value is higher, ~15%, for the 70° case. We note that the film deposited at 70° contains mesopores (2–50 nm),[15] in addition to the ~1 nm nanopores, which may explain the weaker relaxation and support the view that the pore structure is important in determining the polarization.

DISCUSSION

We, here, discuss our proposal that the spontaneous polarization of the ASW films is due to the porosity of the films. We start by considering the surface dipole created when ASW is deposited at low temperatures on unpolarized *crystalline* ice (Fig. 1), based on the simulation results for the growth of an ice cluster done by Buch.[24] The simulations with the ice cluster show that the cluster surface contains a large fraction (119 out of 450) of molecules which are not tetrahedrally coordinated, as in the bulk, but are two- or three-coordinated, due to the limited molecular mobility at low deposition temperatures.[12,24] The most striking feature of the simulation results is the selectivity of the condensation process: a two-coordinated molecule always provides a dangling oxygen atom (d–O, involved in only one hydrogen bond) and a dangling hydrogen atom (d–H, not hydrogen bonded), and a three-coordinated molecule provides either a d–O or a d–H, with a preference to d–O. Such selections result in a predominance of d–O atoms with lone electrons exposed toward the external surface of the cluster, though the origins are not well understood by the simulations yet. These incompletely coordinated surface molecules with unbalanced d–O atoms constitute a thin surface polarized layer with negative polarity, explaining the observed initial abrupt change (~−0.25 V) in the surface potential in the first 5 ML (Figs. 1 and 2(a)) of deposition, where most of the molecules are exposed to either the substrate or the vacuum and cannot engage in the tetrahedral arrangement. These incompletely coordinated molecules at the low coverages form new hydrogen bonds with subsequent impinging molecules, evolving to the tetrahedral arrangement and buried in the bulk; in turn, new unbalanced d–O atoms from the impinging molecules are presented at the film-vacuum interface. Thus, the dipole layer stays at the film-vacuum interface, as indicated in Fig. 7(a) and does not produce a surface potential that changes linearly with film thickness.

As condensation continues, surface protrusions and then pores develop because of shadowing effects,[24] and the above argument about the thin polarized layer at the film-vacuum interface due to unbalanced d–O atoms also applies to walls of the pores (also referred as *internal surface*). Detailed information regarding the shape of the pores is not available yet, we here assume pores with the cylindrical symmetry to reduce the complexity; thus, the transverse component of the surface dipoles on the pore walls, if any, is expected to be cancelled out by those on the opposite side of the walls. We would expect no net film voltage induced by the pores due to the assumed symmetry of the pores, if the surface dipoles are aligned perpendicularly to the internal surface (with only transverse component), resembling those at the film-vacuum interface. However, in

the immediate vicinity of the film-vacuum interface, the d–H (d–O) atoms sticking out of the walls are repelled (attracted) by the external polarized layer, which results in tilted dipoles (TDs) on the walls, contributing to an extra axial component with the more positive end pointing towards the substrate. The tilted dipoles, in turn, induce the similar alignment of the dipoles on the walls. Thus, as condensation continues, the axial component of the tilted dipoles on the walls, unlike the polarized layer at the film-vacuum interface, propagates in the film, which develops an average macroscopic electric field ($\vec{E}$) in the film along the axis of the pores, as shown in Fig. 7(b), and explains the linear growth of the surface potential (V_s) with film thickness (d) (Figs. 1 and 2(a)), since $V_s \sim (-\left|\vec{E}\right| \cdot d)$.

The decreased magnitude of the rates in surface potential changes ($|\Delta V_s/\Delta L|$) at increasing deposition temperature, as shown in Fig. 2(b), is consistent with the TD model proposed above. As the deposition temperature increases, the decrease in porosity[22] reduces the internal surface area, and therefore the tilted dipoles on the internal surface, resulting in a decrease of the $|V_s|$ then the $|\Delta V_s/\Delta L|$. Above ~110 K, thermal depolarization, bulk diffusion, and crystallization change the nature of the problem.[3]

We now determine whether our TD model is consistent with the observed decrease in the IPF with increasing angle of deposition (Fig. 5). One characteristic widely reported for films, especially metal films, grown at low temperatures, is the formation of a columnar structure due to the limited surface diffusion.[25] The columns are oriented toward the vapor beam (at the incidence angle of θ) and form an angle α with respect to the substrate normal. The angle α is universally observed to be somewhat smaller than the angle θ, and the tangent rule, $\tan(\alpha) = 1/2\tan(\theta)$, was observed in metal films by various investigators.[25] For an ASW system deposited at low temperatures with limited surface diffusion, results from the ballistic deposition simulations also suggest a columnar structure with the tilt angle α slightly smaller than the incidence angle θ, though these simulations cannot accurately describe the molecular-scale diffusion of the condensing water molecule and must rely on normalization to experimental porosities.[23]

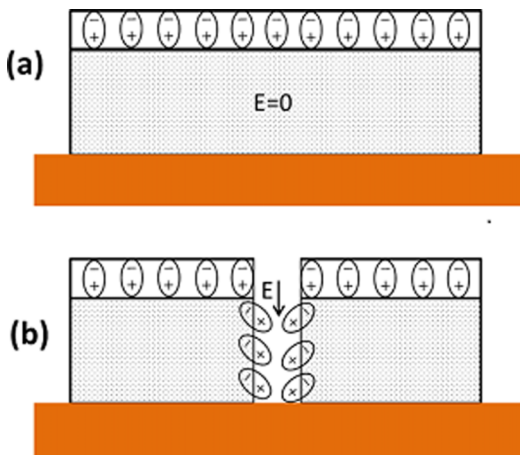

FIG. 7. (a) A thin layer of dipoles that stays at the film-vacuum interface without propagating into the bulk. (b) Tilted dipoles on the walls of a pore result in a net electric field E along the axis of the pores, due to interactions with the dipole layer at the film-vacuum interface.

An important consideration we would like to mention here is that the observed voltage, V_s measured by the Kelvin probe, is only sensitive to the component of polarization *normal* to the film-vacuum interface, $P_\perp$, which decreases as the cosine of the tilt angle α of the columnar structures. As the incidence angle θ increases, the increased internal surface area due to the increased porosity results in an increase of the tilted dipoles and therefore $P_\perp$; however, the increased α with increasing θ results in a decrease of the $P_\perp$, since $P_\perp \sim \cos(\alpha)$. Therefore, if $\alpha \approx \theta$, the expected increase in V_s via increased internal surface area could be offset by the cosine correction for the tilt angle α. A missing parameter in the discussion pertaining to the angular dependence of IPF is the dependence of the pore size on the incidence angle θ, which might cause a decrease in the polarization. Thus, our conclusion is that the observed decrease in the IPF with increasing incidence of deposition in Fig. 5 is a competition between an increase in porosity, tilting of the columnar structure, and a change in the pore size distribution. If the incidence angle θ is randomly chosen from a cosine distribution of angles between 0° and 90°, corresponding to the case for a film deposited from a diffuse background source, the tilt angle α of the microscopic columnar structures is expected to follow the same distribution as θ. It is not surprising that the observed V_s in this case, resulting from the dipole moment averaged over the tilt angles, is close to that of a film deposited at 45°, as shown in Fig. 5.

To enhance the credibility of our proposal and model pertaining to the correlation between the V_s and the microporous structure in ASW, we compared the thermal evolutions of the V_s and the infrared absorption features of the dangling O–H bonds (DB1 at 3720 cm^{-1} and DB2 at 3696 cm^{-1}), known markers of the two- and three-coordinated water molecules on walls of the pores, respectively,[12] and investigated recently by selective IR absorption.[26] Figs. 8(a) and 8(b) show the decreases in $|V_s|$ and the integrated absorbance of the two dangling bonds (DB1 and DB2) in the ASW films during heating from the deposition temperature (10 and 30 K, respectively) to 120 K. Insets in Fig. 8 show the infrared absorption spectra for the films acquired at various heating temperatures. The most striking result is that the DB1 and $|V_s|$ have similar trends of temperature-dependent evolutions. Since DB1 (at 3720 cm^{-1}) is due to two-coordinated surface water molecules,[11,12,26] this observed resemblance strongly supports that the polarization in ASW results from a fraction of aligned two-coordinated molecules on the pore walls and that the decrease in $|V_s|$ during heating, as observed in Figs. 3 and 6, is due to the disappearance of the polarization, which is associated with the disappearance of these incompletely coordinated water molecules with increasing temperature. We notice that the thermal decrease in DB2, at 3696 cm^{-1} and assigned to three-coordinated molecules,[11,12,26] is much smaller, deviating from the evolution of the $|V_s|$ or DB1. One possibility for the observed differences between the thermal evolutions of DB2 and $|V_s|$ is that the three-coordinated molecules do not contribute to the polarization, and no direct correlations between their thermal evolutions are expected. Another explanation for the slower decrease in the DB2, compared to $|V_s|$ or DB1, could be that additional three-coordinated molecules are introduced, as the two-coordinated molecules rearrange

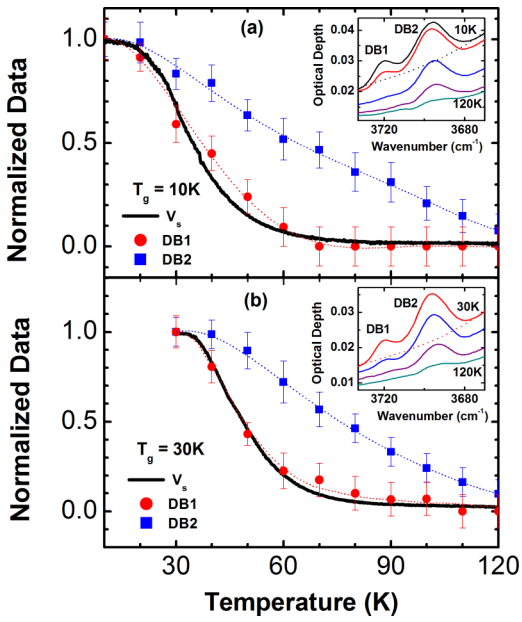

FIG. 8. Comparisons between the surface potential (V_s) and the integrated infrared absorbance of the dangling bonds (DB1, DB2) when heating ASW films (1100 ML) at 1.8 K/min, following deposition at 10 K (a) and 30 K (b) at 45° incidence. V_s, DB1, and DB2 were normalized to values at growth. Inset: infrared absorption spectra of the films (at ~2.7 μm) during heating. The acquired temperatures for the spectra from top to bottom are 10, 30, 60, 90, and 120 K in the inset in (a) and 30, 60, 90, and 120 K in the inset in (b). The integrated absorbance of the dangling bonds DB1 (at ~3720 cm^{-1}, assigned to two-coordinated surface molecules) and DB2 (at ~3696 cm^{-1}, assigned to three-coordinated surface molecules) was calculated after subtractions of the continuous baseline absorption (dashed lines).

towards three-coordinated molecules during heating.[24] If the latter explanation is correct, we could not rule out the possibility that the three-coordinated molecules contribute to the polarization. Therefore, the observed deviation in the evolutions of DB2 and $|V_s|$ in Fig. 8 impedes us in setting a certain correlation between the three-coordinated molecules and the polarization in the ASW films.

CONCLUSION

In conclusion, we propose that the observed intrinsic ASW surface potential results from a fraction of aligned water dipoles on the internal surface area of the pores. We present strong evidence supporting that the incompletely coordinated surface molecules, especially the two-coordinated surface molecules, contribute to the aligned water dipoles. While heating the ASW films, incompletely coordinated molecules evolve towards configurations with higher coordination, which results in depolarization and the decrease in magnitude of the polarization voltage. The effects observed here could have applications for other microporous solids, such as amorphous silica, at higher temperatures.

ACKNOWLEDGMENTS

We acknowledge support from the NASA Outer Planets Research Program (NNS11AM42G). We thank C. Dukes for her discussions and comments on this manuscript.

[1]K. Kutzner, Thin Solid Films **14**, 49 (1972).
[2]L. Onsager, D. L. Staebler, and S. J. Mascarenhas, J. Chem. Phys. **68**, 3823 (1978).
[3]M. J. Iedema, M. J. Dresser, D. L. Doering, J. B. Rowland, W. P. Hess, A. A. Tsekouras, and J. P. Cowin, J. Phys. Chem. B **102**, 9203 (1998).
[4]J. Shi, M. Fama, B. D. Teolis, and R. A. Baragiola, Phys. Rev. B **85**, 035424 (2012).
[5]E. Elliott, T. I. Pritchard, M. J. Hampshire, and R. D. Tomlison, Vacuum **19**, 366 (1969).
[6]J. Chrzanowski and B. Sujak, Thin Solid Films **79**, 101 (1981).
[7]R. Balog, P. Cicman, D. Field, L. Feketeova, K. Hoydalsvik, N. C. Jones, T. A. Field, and J. P. Ziesel, J. Phys. Chem. A **115**, 6820 (2011).
[8]R. Balog, P. Cicman, N. C. Jones, and D. Field, Phys. Rev. Lett. **102**, 073003 (2009).
[9]X. Su, L. Lianos, R. Y. Shen, and G. A. Somorjai, Phys. Rev. Lett. **80**, 1533 (1998).
[10]A. A. Tsekouras, M. J. Iedema, and J. P. Cowin, Phys. Rev. Lett. **80**, 5798 (1998).
[11]B. Rowland and J. P. Devlin, J. Chem. Phys. **94**, 812 (1991).
[12]V. Buch and J. P. Devlin, J. Chem. Phys. **94**, 4091 (1991).
[13]E. Mayer and R. Pletzer, Nature (London) **319**, 298 (1986).
[14]K. P. Stevenson, G. A. Kimmel, Z. Dohnalek, R. S. Smith, and B. D. Kay, Science **283**, 1505 (1999).
[15]U. Raut, M. Fama, B. D. Teolis, and R. A. Baragiola, J. Chem. Phys. **127**, 204713 (2007).
[16]N. J. Sack and R. A. Baragiola, Phys. Rev. B **48**, 9973 (1993).
[17]M. A. Allodi, R. A. Baragiola, G. A. Baratta, M. A. Barucci, G. A. Blake, P. Boduch, J. R. Brucato, C. Contreras, S. H. Cuylle, D. Fulvio, M. S. Gudipati, S. Ioppolo, Z. Kanuchova, A. Lignell, H. Linnartz, M. E. Palumbo, U. Raut, H. Rothard, F. Salama, E. V. Savchenko, E. Sciamma-O'Brien, and G. Strazzulla, Space Sci. Rev. **180**, 101 (2013).
[18]M. S. Westley, G. A. Baratta, and R. A. Baragiola, J. Chem. Phys. **108**(8), 3321 (1998).
[19]A. H. Narten, C. G. Venkatesh, and S. A. Rice, J. Chem. Phys. **64**, 1106 (1976).
[20]C. Bu and R. A. Baragiola, "Ion-induced electrostatic charging and discharging of amorphous solid water films" (unpublished).
[21]J. B. Bossa, K. Isokoski, M. S. de Valois, and H. Linnartz, Astron. Astrophys. **545**, A82 (2012).
[22]B. S. Berland, D. E. Brown, M. A. Tolber, and S. M. George, Geophys. Res. Lett. **22**, 3493, doi: 10.1029/95gl03504 (1995).
[23]Z. Dohnalek, G. A. Kimmel, P. Ayotte, R. S. Smith, and B. D. Kay, J. Chem. Phys. **118**, 364 (2003).
[24]V. Buch, J. Chem. Phys. **96**(5), 3814 (1992).
[25]A. G. Dirks and H. J. Leamy, Thin Solid Films **47**, 219 (1977).
[26]J. A. Noble, C. Martin, H. J. Fraser, P. Roubin, and S. Coussan, J. Phys. Chem. Lett. **5**, 826 (2014).